Terao, T., Matsui, S., & Akasaka, K. (1977) *J. Am. Chem. Soc. 99*, 6136–6138.
Tritton, T. R., & Armitage, I. M. (1978) *Nucleic Acids Res. 5*, 3855–3869.
Yamada, A., Akasaka, K., & Hatano, H. (1978) *Biopolymers 17*, 749–757.
Zhurkin, V. B., Lysov, Y. P., & Ivanov, V. I. (1978) *Biopolymers 17*, 377–412.

Nuclear Overhauser Effect Study of Yeast Aspartate Transfer Ribonucleic Acid†

Siddhartha Roy, Mary Z. Papastavros, and Alfred G. Redfield*

ABSTRACT: Nuclear Overhauser effect studies are described for yeast $tRNA^{Asp}$ in 0.1 M NaCl, pH 7.0. A primary aim is to develop a general method for attacking the problem of assignment in transfer ribonucleic acids (tRNAs). Previously, we have demonstrated the utility of the nuclear Overhauser effect (NOE) between protons on adjacent base pairs combined with C8 deuterium substitution, by assigning the imino protons of the dihydrouridine stem and the two reverse-Hoogsteen base pairs T54-A58 and U8-A14. Here, we extend that approach to other parts of the molecule. We also describe several NOE-connected patterns for, e.g., m^5CG and Ψ55 N3H imino protons which may be of general utility. For the first time, a purine-15–pyrimidine-48 base pair (in this case A15-U48) has been assigned. A total of 13 of 25 base pairs from all parts of the molecule and several noninternally bonded imino protons have now been assigned unambiguously. This is a general method for assigning resonances in tRNA and perhaps in all double-stranded nucleic acids. This, and the distance information inherent in NOE measurements, should make NMR more generally applicable to nucleic acids.

Nuclear magnetic resonance is being applied to an increasing variety of problems of biological interest. We are interested in studying the conformation, dynamics, and structure–function relationship of transfer ribonucleic acid (tRNA)[1] by NMR. We have focused our attention on proton NMR because of its sensitivity and the abundance of protons. In the tRNA NMR spectra, the imino protons resonate considerably downfield from the rest of the protons and form a relatively uncluttered set of lines [reviewed by Schimmel & Redfield (1980) and Reid (1981)]. Observable imino protons are from guanosines and uridines, for which the exchange with the solvent has been slowed down by internal hydrogen bonding or inaccessibility to solvent. Thus, at physiological temperature and solution conditions, most of the imino protons, which are part of the secondary and tertiary structure, contribute resonances in this region. In addition, some imino protons which are not internally hydrogen bonded, but are perhaps partially shielded from solvent, also contribute resonances in the same region. Since each AU and GC pair contributes one resonance to this region, and each GU contributes two, the imino proton spectra collectively reflect contributions from most parts of the molecule. Also, the exchange rates of the imino protons with water are important indicators of the segmental mobility of the molecule in solution and an aid to studies of the effect of different physical parameters on the conformation of the molecule (Johnston & Redfield, 1981b). Despite increased attention and a number of attempts to understand the spectra on the basis of chemical shift theories and fragment studies, assignments of the imino proton spectra remained disputed. The conclusions of earlier papers have been challenged, and serious doubts have been raised about the validity of such procedures in tRNA (Sánchez et al., 1980; Roy & Redfield, 1981).

The nuclear Overhauser effect (NOE) can be viewed as transfer of saturation to a proton nearby in space [see, for example, Johnston & Redfield (1981a)]. The magnitude of transfer is inversely proportional to the sixth power of the distance between the protons and becomes too small to observe beyond 4 Å in most situations. Thus, NOE gives us an important avenue to find the spatial relationship between protons.

NOE is relatively useless unless pairs of resonances it connects can be identified on the basis of uniqueness, chemical modification, isotope labeling, or previously identified NOEs. The first such marker in tRNA was the GU pair (Johnston & Redfield, 1978). GU pairs contain two imino protons in close proximity and hence show a relatively large and unique transfer of saturation pattern between these exchangeable protons. The study of GU pairs has been extended to other tRNAs.

Many other markers were subsequently developed. There are relatively few methyl groups in tRNA, and many of them can be assigned by comparison between tRNAs. Thus, NOE from identified methyl groups to nearby imino protons can identify some important resonances (Tropp & Redfield, 1981; Johnston & Redfield, 1981a). Each AU pair has a purine aromatic proton near in space to the uridine imino proton, so that AU imino protons characteristically show relatively large and sharp NOEs to the aromatic region (Johnston & Redfield, 1981a). In Watson–Crick type AU pairs, the C2 proton of adenosine is close to the uridine imino proton, whereas in

† From the Department of Biochemistry, Brandeis University, Waltham, Massachusetts 02254. *Received May 12, 1982.* This research was partially supported by U.S. Public Health Service Grant GM20168. The NMR facility at the Francis H. Bitter National Magnet Laboratory, MIT, was supported by Grant RR00995 from the Division of Research Resources of the National Institutes of Health and by the National Science Foundation under Contract C-670. A.G.R. is also at the Physics Department and the Rosenstiel Basic Medical Sciences Research Center, Brandeis University.

[1] Abbreviations: tRNA, transfer ribonucleic acid; NOE, nuclear Overhauser effect; EDTA, ethylenediaminetetraacetic acid; T, ribothymidine; m^5C, 5-methylcytidine; Ψ, pseudouridine; ppm, parts per million; BD, benzoylated diethylaminoethyl.

0006-2960/82/0421-6081$01.25/0

reverse-Hoogsteen AU pairs (e.g., U8-A14 and T54-A58), the C8 proton of adenosine is close to the uridine imino proton. Thus, purine C8 deuterated tRNAs could be used to distinguish between Watson–Crick and reverse-Hoogsteen type AU base pairs on the basis of vanished NOEs to the aromatic region (Sânchez et al., 1980; Roy & Redfield, 1981).

In addition to these methods which are based purely on NMR of unmodified tRNAs, chemical modification has been used extensively although it is not relevant to the present work. Resonances correctly assigned in this way include those of the s^4U8-A14 imino proton in *Escherichia coli* tRNAs, the m^7G46 C8 proton, and several methyl groups.

All the NOEs described above are within base pairs and are often large (>15%). NOEs between base pairs, including a tentative imino–imino NOE, were first reported in yeast $tRNA^{Phe}$ (Tropp & Redfield, 1981; Johnston & Redfield, 1981a). They are significantly smaller (~5%) than intra-base-pair effects but have the potential to allow us to hop through the molecule along the helices. This approach has been previously used in smaller proteins (Wagner & Wüthrich, 1979).

We have studied yeast $tRNA^{Asp}$, combining most of the approaches described above, namely, GU pair identification, methyl to imino NOEs, and C8 deuterium substitution, to identify the reverse-Hoogsteen pairs, with analysis of NOEs between protons on adjacent base pairs to yield unambiguous assignment of the imino proton resonance of the dihydrouridine stem and two reverse-Hoogsteen base pairs (Redfield et al., 1981; Roy & Redfield, 1981).

Essentially the same approach has recently been used in an impressive study (Hare & Reid, 1982; Hare, 1982) to identify many resonances at 500 MHz in several tRNAs. The starting points for these studies were several imino resonances identified as near methyl protons, in GU pairs, and by chemical modification. Inter-base-pair NOE is also being increasingly applied to DNA duplexes (Patel et al., 1982a,b).

In the present paper, we extend this approach to further identify resonances in yeast $tRNA^{Asp}$. Resonances from all parts of the molecule have now been identified, and this method is obviously of general utility.

Materials and Methods

Unfractionated yeast tRNA was purchased from Plenum Corp. The crude yeast tRNA was fractionated on a BD-cellulose column (Gillam et al., 1967). Fractions that accepted aspartic acid were pooled together and, after dialysis against H_2O and lyophilization, were applied to another BD-cellulose column, equilibrated at pH 4.0. The procedure of Gillam et al. (1967) was slightly modified for larger scale preparations. The flow rate was 4 mL/h, and 3000 A_{258} units were loaded on a column of size 0.9 × 80 cm. The gradient was 500 mL/500 mL from 0.45 to 0.95 M in NaCl. The fractions that accepted aspartic acid were pooled, dialyzed, lyophilized, applied to a Sepharose 4B column at 4 °C (0.8 × 25 cm), and eluted with a reverse ammonium sulfate gradient [1.3 M in $(NH_4)_2SO_4$ to 0.4 M in $(NH_4)_2SO_4$, 100 mL/100 mL]. Fractions were assayed for aspartic acid acceptance activity and pooled. At this stage, the tRNA usually accepted 1.4 nmol of aspartic acid/A_{258} or greater. The C2 deuterated sample was prepared by the same method from C2 deuterated crude tRNA. Preparation of crude C2 deuterated tRNA will be described in a future communication; briefly, an adenine-requiring mutant of yeast was grown on C2 deuterated hypoxanthine (Sânchez et al., 1980; Roy et al., 1982).

Preparation of samples and NOE experiments were as described by Johnston & Redfield (1981a). The final buffer consisted of 10 mM phosphate, pH 7.5, containing 0.1 M NaCl and 5% D_2O (magnesium was added as described). In some cases where no magnesium was added, 1 mM EDTA was included in the final buffer. Some spectra and NOEs were observed at the Francis H. Bitter National Magnet Laboratory at the Massachusetts Institute of Technology, using essentially the same methods at 500 MHz.

Purified yeast $tRNA^{Asp}$ prepared by a different method (Giegé et al., 1977) was also kindly given to us by Dr. R. Giegé of the Institute de Biologie Moleculiere et Cellulaire, Strasbourg, and was used in the early part of this work.

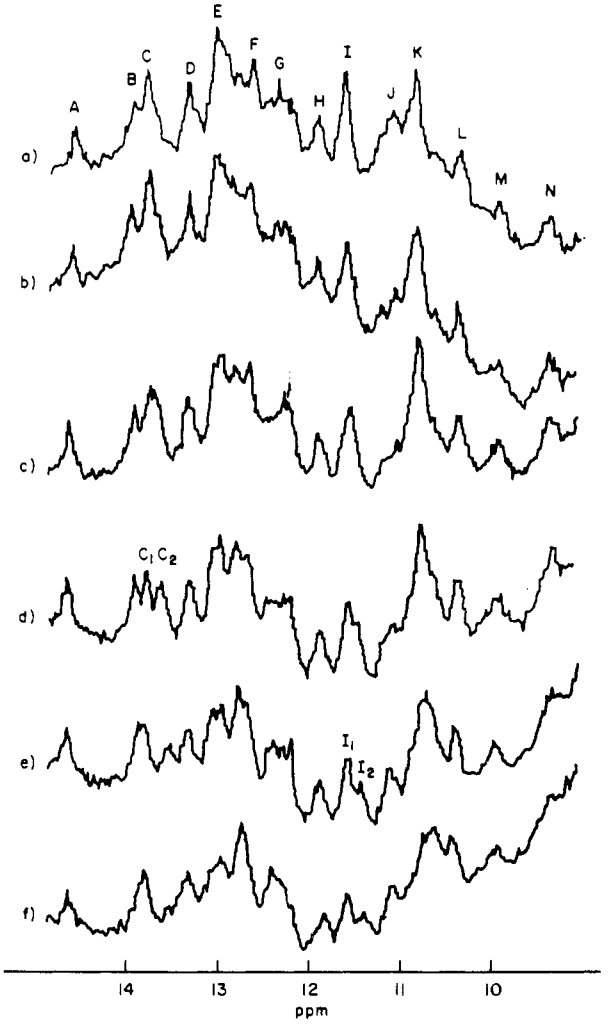

FIGURE 1: Spectra of the imino region of yeast $tRNA^{Asp}$ vs. $MgCl_2$ concentration at 28 °C in 0.01 M phosphate buffer, pH 7.0, containing 0.1 M NaCl. (a) Metal ions have been rigorously removed by dialysis. (b–f) Spectra at Mg^{2+}/tRNA ratios of 1, 2, 4, 8, and 16, respectively.

Results

Spectra vs. Magnesium. It is known that magnesium binds to tRNA and enhances the stability of tRNAs, altering its thermal denaturation profile and other physical properties (Johnston & Redfield, 1981a,b; Crothers & Cole, 1978; Privalov & Filimonov, 1978). A magnesium titration was performed by us with a preliminary aim of identifying magnesium-sensitive peaks and finding the most suitable condition for performing NOE experiments.

Figure 1 presents the results of a magnesium titration (on a sample of yeast $tRNA^{Asp}$). Two major changes are immediately noticeable. Peak C at zero magnesium concentration splits into two peaks, C_1 and C_2, at a Mg^{2+}/tRNA ratio of 4. At an even higher magnesium concentration (Mg^{2+}/tRNA

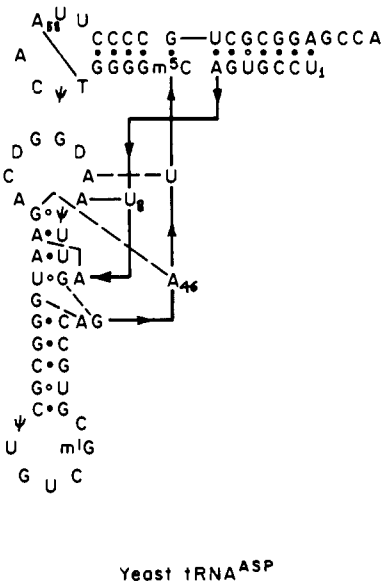

FIGURE 2: Nucleotide sequence of yeast tRNA^{Asp}. The sequence is shown in the form introduced by Kim, to emulate the tertiary structure. Several tertiary interactions expected from preliminary X-ray studies are shown as dashed lines between bases. The two expected reverse-Hoogsteen pairs are shown as lighter solid lines.

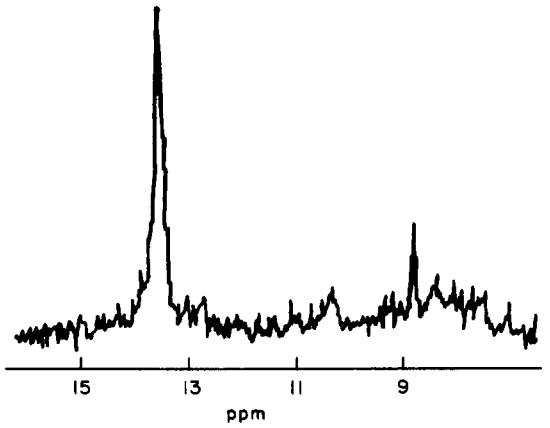

FIGURE 3: NOE study at zero magnesium concentration. The irradiated peak is the shoulder of peak C.

ratio of 8–16), peak C_2 moves further upfield and finally merges with peak D. Peak I also splits into two peaks, I_1 and I_2, at a Mg^{2+}/tRNA ratio of 8. There are also noticeable changes in peaks E, F, and G. Most of the NOE experiments were performed at a Mg^{2+}/tRNA ratio of 4, but some were done at higher or lower magnesium concentrations as described later.

Nuclear Overhauser Effect. (A) AU Pairs. There are seven AU base pairs in this molecule (Figure 2). Two of them, U8-A14 and T54-A58, are reverse-Hoogsteen base pairs and have been identified previously on the basis of C8 deuteration and AU to GU NOEs (Roy & Redfield, 1981). Two more AU pairs, AU11 and AU12, have been identified by similar NOE patterns. All these AU pairs have sharp NOEs to the aromatic region. At 28 °C, there is another sharp NOE from peak C_2 to a peak at 8.79 ppm which presumably comes from another AU pair. Two other possible AU pair NOEs could not be found at this temperature and magnesium concentration. Peak C_2 gives a second NOE at 10.52 ppm. The source of this NOE is the same proton that gives rise to the NOE at 8.89 ppm. This can be clearly seen in a sample containing no magnesium (Figure 3). Since the three remaining unidentified base pairs could be unstable for different reasons

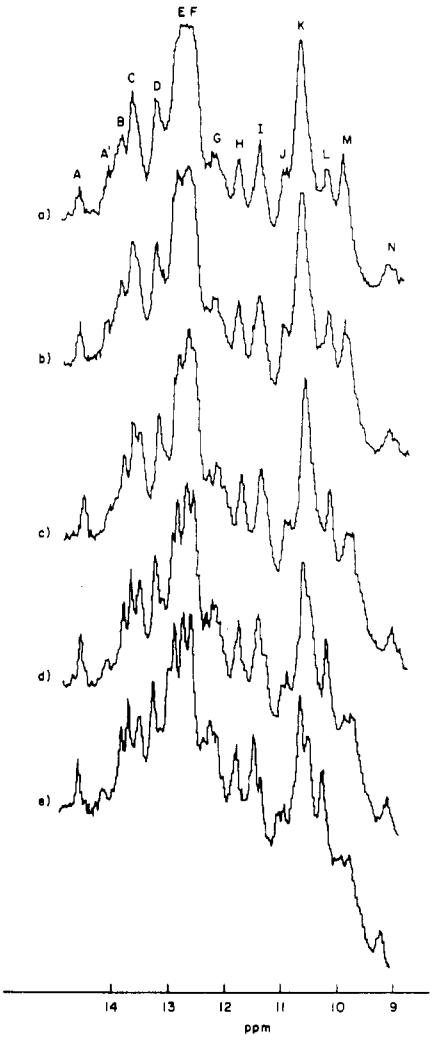

FIGURE 4: Temperature dependence of the imino region spectra of purine C8 deuterated yeast tRNA^{Asp}. The sample had a Mg^{2+}/tRNA ratio of 8. Other conditions were the same as those in Figure 1. (a–e) Spectra taken at temperatures of 12, 16, 20, 28, and 32 °C, respectively.

(A15-U48 is a tertiary base pair; AU1 and AU7 are at the end of a helix), we decided to investigate the spectra and NOEs as a function of temperature at increasing magnesium ion concentrations. Figure 4 shows the effect of temperature on the downfield spectrum of C8 deuterated yeast tRNA^{Asp} at a Mg^{2+}/tRNA ratio of 8. (The reason for choosing the C8 deuterated sample will be made clear below. Nondeuterated yeast tRNA^{Asp} gave similar spectra.) At a lower temperature (<20 °C), there is clear evidence of a new peak at 14 ppm which was absent at lower magnesium concentration and higher temperatures (>20 °C). Irradiation of this peak at 15 °C gives a sharp NOE at 7.4 ppm. In addition, the intensity under peak B (U8-A14) appears increased. Indeed, irradiation of peak B at 15 °C produced a sharp NOE at 7.65 ppm which decreased in size with increasing temperature. Since this NOE is close to that involving the C8 proton of A14 (7.8 ppm), the C8 deuterated sample provided an unambiguous observation of this NOE. At higher field strengths (500 MHz), it was possible to resolve all three resonances (data not shown). So, by varying the temperature and magnesium concentration, combined with NOE, it was possible to detect all seven AU pairs. When peak C_1 was irradiated, in addition to the NOEs already described before (Roy & Redfield, 1981), there was a NOE to a peak at 12.94 ppm. The NOE results are summarized in Table I.

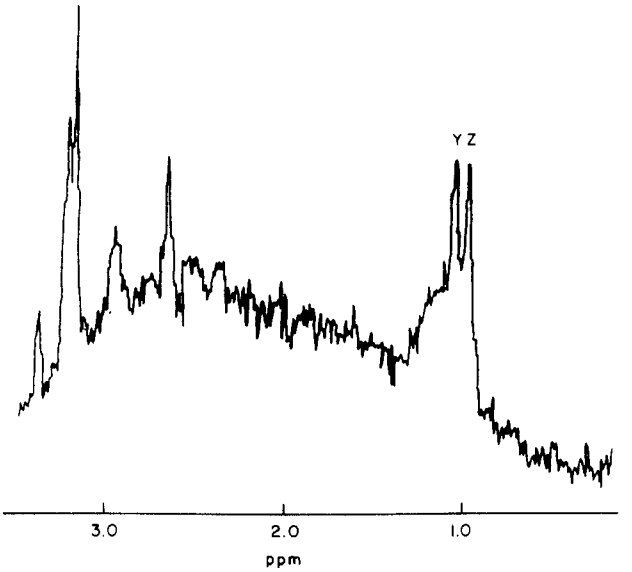

FIGURE 5: Methyl region spectra of yeast $tRNA^{Asp}$ at zero magnesium concentration. The solution composition is the same as in Figure 1. The two most upfield peaks are those of the T54 and m^5C49 as discussed in the text. We see the broad hump under these peaks in many samples of yeast $tRNA^{Asp}$, with varying intensity between samples. We do not know its origin, and we do not find it in other tRNAs. Other peaks are dihydrouridine, m^1G37 methyl, and EDTA resonances.

(*B*) *Methyl Region.* There are three methyl groups in yeast $tRNA^{Asp}$: T54, m^5C49, and m^1G37. Figure 5 shows the methyl region of yeast $tRNA^{Asp}$. It may reasonably be assumed that the two most upfield peaks Y and Z are respectively the m^5C and T methyl resonances. The arguments for these assignments are that in other tRNAs both T and m^5C methyls resonate in this region (Tropp & Redfield, 1981; Kan et al., 1977). Also NOE patterns from these peaks are very similar to NOE patterns from assigned T and m^5C peaks in other tRNAs, e.g., yeast $tRNA^{Phe}$ (Tropp & Redfield, 1981; S. Roy and A. G. Redfield, unpublished experiments). When peak Z (which is presumably the T54 methyl) was irradiated, there were two NOEs to the imino region, one at 10.73 ppm and another at 11.54 ppm. The former NOE is about 7% in size whereas the latter is much smaller. However, the latter can be readily confirmed with longer preirradiation (500 ms). The size of the NOE at 11.54 ppm showed a strong dependence on preirradiation time. Peak Z has also two sharp aromatic NOEs at 7.54 and 6.85 ppm. The latter disappears on C8 deuteration.

Peak Y when irradiated gives rise to one NOE at 13.02 ppm. Peak Y also gives another major NOE at 7.41 ppm. The summary of these NOE results is shown in Table I.

(*C*) *GU Pairs.* Among the three GU and one GΨ pairs present in this tRNA, we have already identified GU10 and GΨ13. When peak I is irradiated, in addition to the NOE to peak L which was identified as GΨ13, there is a NOE to peak K at 10.82 ppm. The magnitude of the NOE is 10–15%. Peak I, when irradiated, also gives three NOEs in the aromatic region, at 8.79, 8.4, and 7.8 ppm, of magnitudes 5%, 10%, and 10%, respectively. The latter two vanish on purine deuteration. Irradiation of peak K produces one NOE to peak H (25%) at 11.84 ppm which has already been assigned to GU10 and another to peak I at 11.50 ppm. There is also a major NOE to the aromatic region at 7.39 ppm. This NOE is probably to a pyrimidine aromatic proton because it does not disappear on purine C8 or C2 deuteration. Peak K also has a smaller NOE to peak A which has already been assigned. Peak L, when irradiated, gives an NOE to peak K at 11.44 ppm (25%) and 13.88 ppm (~7%), both of which have been assigned to GΨ13 and U8A14, respectively. In addition, NOEs were observed at 8.79 ppm (15%) and 9.38 ppm (~10%), the former of which vanishes on C2 deuteration. Peak M, when irradiated, shows an NOE to peak K at 10.66 ppm (~20%). Peak N has an NOE to peak C_2 (~10%). All of these NOEs are summarized in Table I.

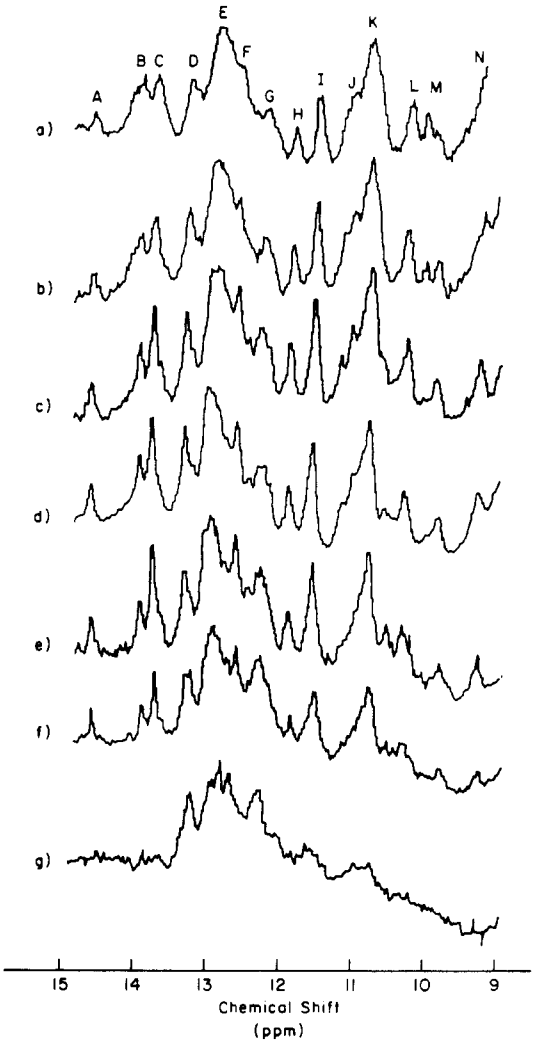

FIGURE 6: Temperature dependence of the imino region spectra of yeast $tRNA^{Asp}$ at zero magnesium concentration. (a–g) Spectra taken at 8, 14, 23, 28, 34, 38, and 44 °C, respectively.

Melting Studies on Yeast $tRNA^{Asp}$. This preliminary study was carried out at zero magnesium ion concentration. The result of the melting study is shown in Figure 6. When the temperature is raised from 8 to 34 °C, peak B loses substantial intensity, estimated to be equivalent to two protons. The other peaks that melt early include a peak between M and L and possibly a part of peak K. From 34 to 44 °C, peaks A, B, C, H, J, L, M, and N melt completely. Large parts of peaks I and K melt, but some intensity remains at 44 °C.

Discussion of Assignments

We now consider the assignments of the resonances to protons in the structure. We emphasize that in making these assignments we have made the following assumptions, none of which involve calculation of resonance positions from a given structure. The assumptions are the following: (1) The overall folding pattern of yeast $tRNA^{Asp}$ is roughly similar to that of yeast $tRNA^{Phe}$. This assumption is supported by the work of Moras et al. (1980), who obtained the 3.5-Å resolution X-ray

Table I: Summary of NOE Data[a]

peak irradiated	assignment	position (ppm)	NOE position (ppm)	fractional transfer	NOE assignment
A	AU11 (U11 N3)	14.6	7.9[b]	0.3	A24 C2
			10.7	0.07	GU10
			11.85	0.05	GU10
			13.8[c]	0.05	U12 NB
A′	AU1 or -7 (U N1)	14.1	7.4[d]	0.015	AU1 or -7 (A C2)
B	U8-A14 (U8 N3)	13.9	7.8[e]	0.151	A14 C8
			10.3	0.07	GΨ13
			11.54	0.05	GΨ13
			7.65[f]	0.2	AU1 or -7 (A C2)
C_1	T54-A58 (T54 N3)	13.75[g]	8.4[e]	0.15	A58 C8
			12.95	0.05	G53 N1
C_2	AU12 (U12 N3)	13.6[g]	7.5[b]	0.2	A23 C2
			7.9	0.1	A24 C2
			9.3	0.1	GΨ13 noninternally bonded NH
C_2	A15-U48 (U48 N3)	13.6	8.8[b]	0.2	A21 C2
			10.5	0.05	U594 N3
E	GC53	12.95	13.75	0.05	T54 N3
H	GU10	11.85	10.7	0.25	GU10
I	GΨ13	11.5	10.3	0.25	GΨ13
			7.8[b]	0.07	A14 C8
			8.8	0.05	A21 C2
I	GU5 or -40	11.5	8.4[b]	0.05	A58 C8
I	Ψ55 N3H	11.5	8.4[b]	0.05	A58 C8
K	GU10	10.8	11.85	0.25	GU10
			14.6	0.05	U11 N3
K	Ψ55 N1	10.8	7.4	0.5	Ψ55 C6
K	GU5 or -40	10.8	11.5	0.15	GU40 or -5
K	GU5 or -40	10.8	9.8[f]	0.15	GU5 or -40
L	GΨ13	10.3	11.5	0.25	GΨ13
		10.3	8.8[b]	0.15	A21 C2
		10.3	9.3	0.05	Ψ13 noninternally bonded NH
M	GU5 or -40	9.8	10.65	0.15	GU5 or -40
N	Ψ13 N1 or -3	9.3	13.5[h]	0.1	AU12 N3
			10.3	0.05	GΨ13
Z	T54 methyl	0.95	10.7	0.08	Ψ55 N1
			11.5[i]	0.05	Ψ55 N3
Y	m^{5}C49 methyl	1.05	13.0	0.05	G65 N1

[a] All NOEs found with identical positions and intensities at both zero Mg^{2+} concentration and 4 mM Mg^{2+} and 28.5 °C except as indicated. Other buffer conditions are given in the text. All magnesium concentrations refer to added magnesium, and tRNA concentrations were 1 mM. Volume change due to addition was negligible. [b] Vanishes on purine C2 deuteration. [c] At zero magnesium concentration. In 4 mM magnesium, the NOE was at 13.5 ppm. [d] Observed only at 6 mM Mg^{2+} and 16 °C. [e] Vanishes on purine C8 deuteration. [f] Observed only below 20 °C and 4 mM magnesium or higher. [g] C_1 and C_2 overlap at 13.7 ppm in zero Mg^{2+}. [h] At 6 mM magnesium. In zero magnesium concentration, the NOE was at 13.7 ppm. [i] Preirradiation time = 500 ms.

structure of yeast tRNA^{Asp} and found it similar to that of yeast tRNA^{Phe} except for one important difference (absence of the G19–C56 tertiary interaction) not relevant to the assignments made here. (2) The most downfield peaks represent AU base pairs, whereas GU base pairs and noninternally bonded imino protons resonate around 9–12.5 ppm. This assumption is supported by the fact that all the NOEs from the most downfield region to the aromatic region vanish on purine C2 and C8 deuteration, as expected for Watson–Crick and reverse-Hoogsteen AU base pairs, respectively. GU pairs are also well investigated and have generally been assigned in the 9–12.2-ppm range (Johnston & Redfield, 1978).

We assume there is either a unique conformation for this tRNA in solution or at least a structure that is the rapid time average of similar conformations. By our NMR studies, we find no evidence for slow or strongly temperature-dependent conformation changes (slow on a time scale of $\sim 10^{-3}$ s). Minor temperature dependence that we see in the NMR spectrum can be explained by relatively rapid solvent exchange for certain imino protons at the ends of helical stems.

Assignment of the D Stem and Two Reverse-Hoogsteen Base Pairs. As described previously (Roy & Redfield, 1981), two reverse-Hoogsteen pairs were identified at peaks B and C_1 by the criterion of vanishing NOE in a C8 deuterated tRNA. One of these resonances (peak B) has a small NOE to peaks I and L already identified as a GU-type pair. Since U8-A14 is stacked above GΨ13 and there are no GU pairs around T54-A58, U8-A14 was assigned to peak B. Peak A, which was determined to be a single proton, gives an NOE to resonances of another GU pair, namely, peaks H and K, and to another AU imino resonance, peak C_2. The other AU and GU pair close in space is AU11 and GU10. Hence, AU11 was assigned to peak A, and GU10 to peaks H and K, and AU12, the only other AU pair close in space to AU11, was assigned to peak C_2.

Assignment of Other AU Pairs. Among the three remaining AU base pairs, A15-U48, AU7, and AU1, we have assigned the tertiary A15-U48 to peak C_2 (distinct only at a Mg^{2+}/tRNA ratio of 4). The argument is the following: Peak C_2 has an NOE at 8.8 ppm that vanishes on C2 deuteration, identifying the peak at 8.8 ppm as an adenine C2. Peak L, to which one proton of GΨ13 was assigned, gives an NOE at 8.8 ppm which also vanishes on C2 deuteration. Since it is possible that another proton, which has the same chemical shift as GΨ13 (peak L), is the source of the NOE at 8.8 ppm, we irradiated peak I, the other half of the GΨ imino pair. Indeed,

when peak I was irradiated, there is a small NOE at 8.8 ppm (~5%), consistent with a second-order NOE through the GΨ proton at peak L (the intensity of a second-order NOE should be the product of two first-order NOEs which in this case would be 0.25 × 0.15 = 0.0375). To prove that both NOEs to 8.8 ppm are to a single proton, we have calculated the area of the proton peak at 8.8 ppm. This peak is separated from the bulk of the aromatic and imino protons, and the area can readily be determined as that of a single proton. Thus, the base pair GΨ13 and peak C_2 (the imino proton which is the source of the 8.8-ppm NOE) are close in space and are connected by an NOE through an adenine C2 proton (8.8 ppm). Among the three unassigned base pairs, A15-U48, AU7, and AU1, only A15-U48 is close enough to give such NOE patterns. Hence, A15-U48 is assigned at peak C_2. Since in yeast $tRNA^{Phe}$ the corresponding base pairs G15-C48 and GC13 are separated by a distance of ~7 Å, the question may be raised whether the assignment is a reasonable one. There could be two explanations: One is that the conformation in that region could be different from that of yeast $tRNA^{Phe}$ and A15-U48 and GΨ13 are considerably closer. A second explanation is that the NOE at 8.8 ppm is not that of C2 of A15, but belongs to A21, the base which stacks in between the corresponding base pairs GC13 and G15-C48 in yeast $tRNA^{Phe}$. We have calculated the distance from A21 to GC13 and G15-C48 and found them to be within 4 Å. We favor the second explanation because the NOEs between other base pairs indicate that the conformation of the D stem and U8-A14 is similar to that of the yeast $tRNA^{Phe}$ crystal structure.

This raises the question why is the NOE from the imino proton of U48 to the proton of A15 not seen. There may be several explanations. It may be quite small, or it may be hidden under a bigger NOE, or the base pair, which is not a standard Watson–Crick type, could be formed such a way that the distance between N3H of U48 and C2H of A15 is large. In fact, we have not seen NOEs from all AU imino protons to the aromatic region in several instances [e.g., yeast $tRNA^{Phe}$; see Johnston & Redfield (1981a)].

There is also another NOE from A15-U48 to a peak at 10.5 ppm. This is certain to be an imino proton. The most likely candidate for this peak is U59 which is hydrogen bonded to G15-C48 in the yeast $tRNA^{Phe}$ crystal structure. Thus, the resonance at 10.5 ppm is assigned to the U59 imino proton.

That leaves peak A′ and the proton at peak B which is the source of the NOE at 7.65 ppm, which must be AU7 and AU1. Both are temperature sensitive. At this point, it is not possible to say which of these two peaks belongs to which base pair.

GU Pairs. GU pairs can be distinguished from AU and GC pairs by a simple NOE criterion: GU pairs have two imino protons, one contributed by G and the other contributed by U, in close proximity (~2.5 Å). Thus, this is the only kind of base pair that shows a large (15–30%) NOE between two imino protons. A number of tRNAs containing GU pairs have been studied and found to have GU imino protons in the range 10–12 ppm. There are three GU and one GΨ pairs in yeast $tRNA^{Asp}$, and we have detected all four by the criterion mentioned above. The pairs of imino proton resonances that have been found to be connected by large saturation transfer are HK, IK, IL, and KM. HK and IL have already been assigned to GU10 and GΨ13, respectively, so pairs IK and KM must be GU5 and GU40. The GU pair represented by KM seems to be highly temperature dependent. The NOEs can only be observed at a Mg^{2+}/tRNA ratio >4 and a temperature <20 °C. Since the size of an NOE is inversely proportional to the relaxation rate of the observed proton, the temperature effect is probably a reflection of increased chemical exchange, hence shorter relaxation time.

Studies on yeast $tRNA^{Phe}$ in zero Mg^{2+} concentration indicate that the acceptor stem resonance melts early, whereas the anticodon stem probably melts at considerably higher temperature. This pattern seems to hold true for the two acceptor stem resonances AU7 and AU1 which melt early in yeast $tRNA^{Asp}$. Thus, peak MK, which shows an increased exchange rate, may be GU5. As we will see later, melting studies at higher temperatures support this hypothesis.

GC Pairs. We have positively identified imino resonances of two secondary GC pairs. There are three methyl groups in this molecule, those of T54, m^5C49, and m^1G. Peak Z is certainly the T methyl on the basis of comparisons with NOE patterns to be described later (Tropp & Redfield, 1981). When peak Y (methyl region) is irradiated, there is one sharp NOE at peak E_1. We identify this as an NOE between the m^5C49 methyl proton and the m^5CG49 imino proton propagated via the external amino group of cytosine-49. Peak Y is almost certainly the m^5C49 methyl because m^5C methyls usually resonate in this position and the NOE pattern from a number of m^5C-containing tRNAs is nearly the same (S. Roy and A. G. Redfield, unpublished experiments). It could be argued that this NOE represents transfer between the m^5C methyl and the adjacent GC base pair imino protons. But in yeast $tRNA^{Phe}$, where m^5CG pairs are situated between AU pairs, similar NOEs are observed (S. Roy and A. G. Redfield, unpublished experiments). In addition, the distance between the methyl protons of m^5C and the nearest amino proton is approximately 2.5 Å, and the distances between the two amino protons, and between the nearest amino proton of m^5C and the imino proton of the base pair, are also small, making this third-order NOE possible.

Peak E_2 is assigned to GC53 on the basis of the NOE from peak C_1. Since peak C_1 is T54-A58, the assignment is straightforward. There is no other GC imino proton near T54-A58.

Other Imino Protons. The NOE pattern from the T methyl resonances has been investigated in detail (Tropp & Redfield, 1981). When peak Z is irradiated, it produces an NOE pattern very similar to the one described by Tropp and Redfield. Peak K is assigned to the Ψ55 N1H because it is in the same region where similar NOEs were observed from the T methyl in other tRNAs and assigned to Ψ55 N1H. The large NOE from peak K (a pyrimidine NOE, because it does not vanish on C2 or C8 deuteration) fits into the pattern Ψ55 N1H to Ψ55 C6H. We observe another weaker NOE from the T methyl to the imino region at peak I. We assign this peak to Ψ55 N3H because there is no other imino proton near the T methyl. Our assignment is bolstered by the fact that there is an NOE from peak I to the aromatic region at 8.4 ppm. This NOE vanished on C8 deuteration and hence can be assigned to C8 of A58. Indeed, in the yeast $tRNA^{Phe}$ crystal structure, Ψ55 N3H and A58 C8H are within 3.5 Å of each other.

We assign peak N to the Ψ13 noninternally bonded NH proton. There is an NOE from peak N to peak C at zero magnesium concentration, and vice versa. This NOE moves upfield exactly like peak C_2 (AU12) as the magnesium concentration is increased gradually. Thus, an imino proton resonating at N is spatially close to AU12 (Mg^{2+}-sensitive peak C_2). The only such imino proton that has not been assigned yet is the Ψ13 NH (noninternally bonded). This is further confirmed by a weaker NOE from peak N to peak L, which is one of the imino protons of GΨ13. Our experiments do not

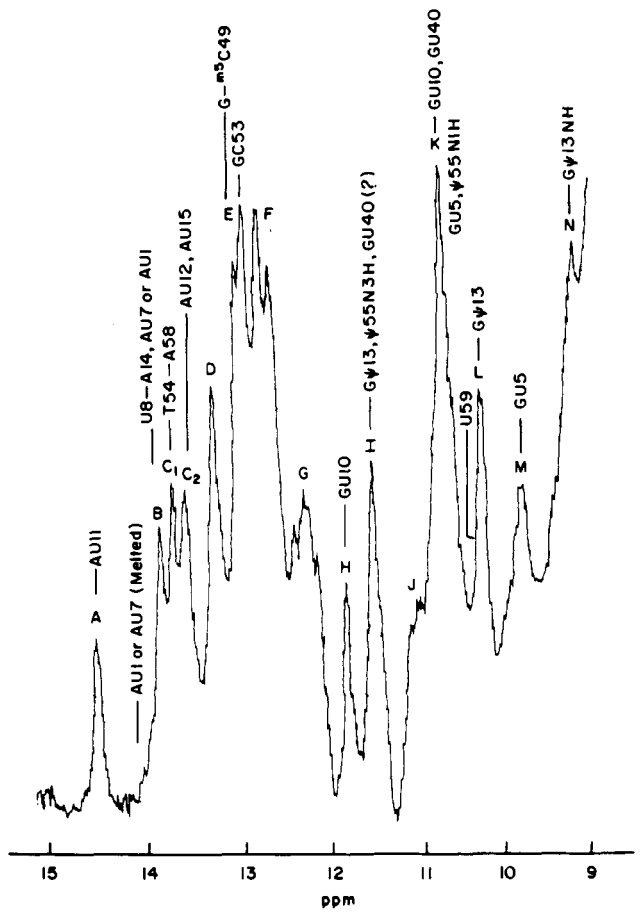

FIGURE 7: NMR spectra of yeast tRNA^{Asp} at a Mg^{2+}/tRNA ratio of 4. Other conditions are the same as in Figure 1. The assignments given here are discussed in the text.

yet permit us to say which NH proton of Ψ13 is internally bonded.

A summary of our assignments is shown on Figure 7. Most of our assignments are based on unambiguous NOE evidence and supported by selected deuteration experiments.

Conclusions

Magnesium is known to affect the structure of tRNAs dramatically. There are changes in the NMR spectra as magnesium binds to the tRNA (Johnston & Redfield, 1981a,b). We have studied the dependence of imino region spectra vs. magnesium concentration to determine the optimum concentration of Mg^{2+} which gives the most resolved spectra. There are several magnesium-sensitive peaks in this tRNA. Two of them can be assigned unambiguously to two D-stem imino protons, AU12 and GΨ13. This is consistent with a magnesium binding site at the bend of phosphate 8. These and other movements in the GC region make the spectra better resolved at a Mg^{2+}/tRNA ratio of 4 at 28 °C. Thus, this condition was chosen for critical NOE experiments.

The spectral position of the two reverse-Hoogsteen base pairs in this tRNA, T54-A58 and U8-A14, is now firmly established. The position of T54-A58 seems to vary little in different tRNAs in which it has been assigned (yeast tRNA^{Phe}, S. Roy and A. G. Redfield, unpublished experiments; *E. coli* tRNA^{Val}, B. R. Reid et al., unpublished experiments). A tertiary pair, A15-U48, is also assigned, and U59 which interacts with A15-U48 is also assigned. Despite the differences seen by X-ray crystallography in D-loop and TΨC-loop interactions, we conclude that the A21–A15–U48–U59 interaction is almost identical in this tRNA, as derived by NOE studies, with that for yeast tRNA^{Phe}. The major difference between yeast tRNA^{Asp} and yeast tRNA^{Phe} seen in X-ray crystallography is in the region of the G19–C56 and G18–Ψ55 interactions (Moras et al., 1980), and we have no assignment of these two base pairs.

Also, for the first time, we have identified the resonance of Ψ55 N3H in a tRNA. This imino proton resonates ~1 ppm downfield of Ψ55 N1H, and this shift is consistent with the idea that it is bonded to a phosphate as seen in the X-ray structure of yeast tRNA^{Phe}. This imino proton has been identified in two more tRNAs and is found to resonate at about 11.5 ppm (yeast tRNA^{Phe}, S. Roy and A. G. Redfield, unpublished experiments; yeast tRNA^{Val}, E. Schejter and S. Roy, unpubished experiments).

The method we have used to identify the imino resonances of the m^5CG base pairs is of general utility. Resonances of m^5CG pairs have been identified in the same way in yeast tRNA^{Phe} (S. Roy and A. G. Redfield, unpublished experiments).

The melting study was a preliminary attempt to determine the thermal stability of different parts of the molecule. Apart from thermolability of acceptor stem resonances mentioned before, two grossly different stable parts of the molecule are evident. At 44 °C, the AU pairs are melted, indicating melting of the acceptor, DHU, and tertiary resonances. GU10, GΨ13, and the GU pair represented by peak MK are melted. The only intensity about 10–12 ppm that remains is under peaks K and I. That would be consistent with IK being GU40 (anticodon stem). Indeed, a large portion of the GC region remains intact (the TΨC and anticodon stems are largely GC). Further studies are in progress, using these resonance assignments, to clarify the structural transitions that occur at higher temperatures.

We have made enormous progress in spectral identification with two other tRNAs, namely, yeast tRNA^{Phe} and yeast tRNA^{Val}. In addition, by using these general techniques at 500 MHz, Hare has identified an overwhelming majority of resonances in *E. coli* tRNA^{Ile} (Hare, 1982).

Finally, we would like to mention that our identifications in yeast tRNA^{Asp} are not in agreement with predictions made with the aid of ring-current shift theory (Robillard et al., 1976). The assignment of resonances guided by ring-current shift theories is questionable, at least as it has been done in the past.

Acknowledgments

We thank Dr. Richard Giegé and his co-workers for the gift of yeast tRNA^{Asp} which initiated the study. We thank Valentina Sánchez for excellent assistance in isolating C8 deuterated yeast tRNA^{Asp}. We also thank Dave Ruben and Ron Haberkorn for helping us to use the NMR facility at the Francis H. Bitter National Magnet Laboratory at the Massachusetts Institute of Technology.

References

Crothers, D. M., & Cole, P. E. (1978) in *Transfer RNA* (Altman, S., Ed.) pp 196–247, MIT Press, Cambridge, MA.

Giegé, R., Moras, D., & Thierry, J. C. (1977) *J. Mol. Biol. 115*, 91–96.

Gillam, I., Millward, S., Blew, D., Tigerstorm, M., Wimmer, E., & Tener, G. M. (1967) *Biochemistry 6*, 3043–3056.

Hare, D. R. (1982) *Biophys. J. 37*, 82a.

Hare, D. R., & Reid, B. R. (1982) *Biochemistry 21*, 1835–1842.

Johnston, P. D., & Redfield, A. G. (1978) *Nucleic Acids Res. 5*, 3913–3927.

Johnston, P. D., & Redfield, A. G. (1981a) *Biochemistry 20*, 1147-1156.
Johnston, P. D., & Redfield, A. G. (1981b) *Biochemistry 20*, 4005.
Kan, L. S., Ts'o, P. O. P., Von der Haar, F., & Cramer, F. (1977) *Biochemistry 16*, 3143-3154.
Moras, D., Comarmond, M. B., Fischer, J., Weiss, R., Thierry, J. C., Ebel, J. B., & Giegé, R. (1980) *Nature (London) 288*, 669-674.
Patel, D. J., Pardi, A., & Itakura, K. (1982a) *Science (Washington, D.C.) 216*, 581-589.
Patel, D. J., Kozlowski, S., Nordheim, A., & Rich, A. (1982b) *Proc. Natl. Acad. Sci. U.S.A. 79*, 1413-1417.
Privalov, P. L., & Filimonov, V. V. (1978) *J. Mol. Biol. 122*, 447-464.
Redfield, A. G., Roy, S., Sânchez, V., Tropp, J., & Figueroa, N. (1981) in *Biomolecular Stereodynamics* (Sarma, R. H., Ed.) pp 195-208, Adenine Press, Guilderland, NY.
Reid, B. R. (1981) *Annu. Rev. Biochem. 50*, 969-996.
Robillard, G. T., Hilbers, C. W., Reid, B. R., Gangloff, J., Dirheimer, G., & Shulman, R. G. (1976) *Biochemistry 15*, 1883-1889.
Roy, S., & Redfield, A. G. (1981) *Nucleic Acids Res. 9*, 7073-7083.
Roy, S., Papastavros, M. Z., & Redfield, A. G. (1982) *Nucleic Acids Res.* (in press).
Sânchez, V., Redfield, A. G., Johnston, P. D., & Tropp, J. (1980) *Proc. Natl. Acad. Sci. U.S.A. 77*, 5959-5662.
Schimmel, P. R., & Redfield, A. G. (1980) *Annu. Rev. Biophys. Bioeng. 9*, 181-221.
Tropp, J., & Redfield, A. G. (1981) *Biochemistry 20*, 2133-2140.
Wagner, G., & Wüthrich, K. (1982) *J. Mol. Biol. 155*, 347-366.

Biosynthesis of Glycosaminoglycans by Thymic Lymphocytes. Effects of Mitogenic Activation†

Gerald W. Hart

ABSTRACT: The immune response is regulated by cellular interactions involving thymus-derived lymphocytes. Even though evidence from several systems suggests that proteoglycans or their polysaccharide side chains, the glycosaminoglycans, are important mediators (modulators) of cellular interactions, little is known concerning the biosynthesis or possible functions of these macromolecules in lymphocytes. As an initial step in our systematic analyses of the complex arrays of protein saccharides of lymphocytes, the biosynthesis and secretion of glycosaminoglycans by both unstimulated and mitogenically activated lymphocytes have been investigated. Isolated thymic lymphocytes were labeled with D-[6-^{3}H]-glucosamine and $^{35}SO_4^{2-}$, and the amounts of radioactivity in each family of glycosaminoglycan or other types of saccharides were determined. The data indicate the following: (1) Lymphocytes synthesize and secrete substantial amounts of glycosaminoglycans. (2) Activated lymphocytes have greatly accelerated rates of secretion of glycosaminoglycans, which appear to be more highly sulfated than those of nonstimulated cells. (3) Sulfated glycosaminoglycans of lymphocytes consist largely of chondroitin 4-sulfates, with smaller amounts of heparan sulfates. (4) Lymphocyte stimulation results in a rapid and dramatic increase in the relative proportion of both cell-associated and cell-secreted chondroitin 6-sulfates. (5) Lymphocytes synthesize large proportions of an apparently unsulfated, glycosaminoglycan-like glycoconjugate which is resistant to sequential treatments degrading all known types of glycosaminoglycans. Taken together with previous work which indicates that exogenously added glycosaminoglycans are capable of altering lymphocyte functions, these data suggest that lymphocyte-derived glycosaminoglycans themselves may play an important role in modulating the cellular interactions which regulate the immune system.

Thymus-derived lymphocytes are now known to regulate both cellular and humoral immune responses via specific cellular interactions with the other cellular components of the immune network (Katz, 1977). Evidence has suggested that the cell-surface saccharide moieties on lymphocytes might play essential roles in mediating these important regulatory cellular interactions (Gesner & Ginsburg, 1964; Gesner, 1966; Yachin, 1975; McKenzie et al., 1977; Kieda et al., 1978; Decker, 1980; Higgins et al., 1980; Muchmore et al., 1980). In fact, lymphocytes can be quantitatively separated into functional subclasses on the basis of the types of terminal saccharides exposed on their cell surfaces (Reisner et al., 1976a,b; Kimura et al., 1979; Mishell & Shiigi, 1980). Recently, I have directly shown that asparagine-linked oligosaccharides on the surfaces of stimulator splenic lymphocytes are required for the allogeneic stimulation of thymic lymphocytes to occur (Hart, 1982), and Black and co-workers have presented evidence for the involvement of asparagine-linked saccharides in the lymphocyte-mediated, *H-2* restricted cytolysis of virus-infected cells (Black et al., 1981).

Allogeneic, antigen- or lectin-induced blast transformation of lymphocytes produces rapid and profound alterations in the surfaces of these cells such as changes in permeability to cations (Quastel & Kaplan, 1968; Parker, 1974), unmasking or an increase in the number of cell-surface receptors (McCune et al., 1975; Miller et al., 1975), altered membrane fluidity (Yahara & Edelman, 1975), dramatic increase in the cell's net negative surface charge (Sato et al., 1979), increased kinase activity, and extensive alterations in saccharide surface topography, as determined by lectin binding [Speckart et al.

† From the Department of Physiological Chemistry, The Johns Hopkins University School of Medicine, Baltimore, Maryland 21205. *Received May 27, 1982.* This work was supported by National Institutes of Health Grant HD 13563 and in part by American Cancer Society Institutional Research Grant No. 1N-11R.

0006-2960/82/0421-6088$01.25/0